# Virus-Incorporated Biomimetic Nanocomposites

Subjects: Nanoscience & Nanotechnology | Engineering, Biomedical | Materials Science, Biomaterials
Contributor: Dong-Wook Han

Owing to the astonishing properties of non-harmful viruses, tissue regeneration using virus-based biomimetic materials has been an emerging trend recently. The selective peptide expression and enrichment of the desired peptide on the surface, monodispersion, self-assembly, and ease of genetic and chemical modification properties have allowed viruses to take a long stride in biomedical applications.

Keywords: virus ; tissue regeneration ; biomimetic nanocomposites ; phage display

## 1. Virus-Based Nanoparticles

Many plants and phage-based viral nanoparticles have been employed so far for tissue regeneration. Plant viral nanoparticles are mono-dispersed, meta-stable, and structurally uniformed [1]. Li revealed that when the virus-based nanoparticle is more robust, the functional nanostructure is more stable, but at the same time they might be harmful to the encapsulated cargo [2].

Though the unmodified TMV nanoparticles have the potential to accelerate osteogenic differentiation in adult stem cells, the lack of affinity to the mammalian cell surface diminishes the cell adhesion property. Hence, the researchers opt for either genetic or chemical modification in viral nanoparticles in order to increase the cell binding capacity and find versatile biomedical applications. Sitasuwan et al. [3] modified the surface of a TMV nanoparticle by coupling azide-derivatized Arg-Gly-Asp-(RGD) tripeptide with tyrosine residues through Cu (I) catalyzed azide-alkyne cycloaddition reaction. When incorporated into the artificial scaffold, the RGD peptides overexpressed on ECM increase initial cell attachment by binding integrin receptors. The spacing between RGD motifs alter biological events, such as fibroblast adhesion and spreading (˂440 nm), focal adhesion assembly (˂140 nm), and induction of stress fiber formation (˂60 nm). Owing to lack of mammalian cell infectivity, cost-effectiveness, and highly uniform size, plant viral nanoparticles have gained attention among nano and biomedical researchers. The Tobacco Mosaic Virus (TMV) constitutes a rod-like shaped nanoparticle with a diameter of 18 nm and length of 300 nm. The TMV nanoparticle consists of a capsid with 2130 identical coat protein subunits, which are responsible for assembling into a helical structure around the ssRNA. When each subunit is modified, the resulting TMV is a polyvalent nanoparticle. The TMV can withstand temperatures up to 60 °C and can be stable in a pH range of 2–10. The TEM micrograph of wild type TMV is shown in Figure 1a [4].

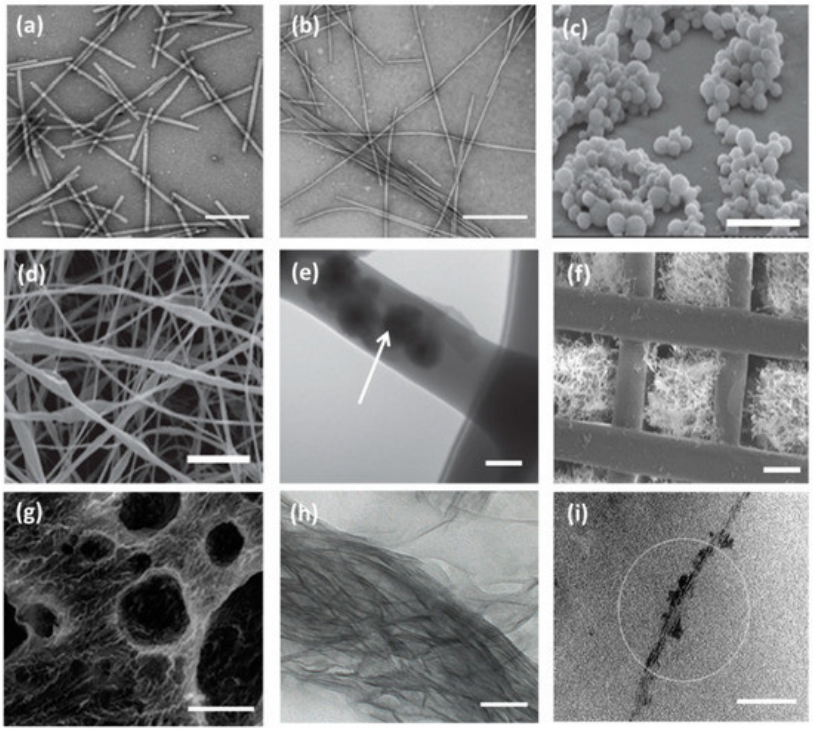


**Figure 1.** TEM micrographs of wild type Tobacco Mosaic Virus (TMV) nanoparticles, scale bar 200 nm (**a**) and TMV/PANI/PSS nanofiber (**b**) generated by flow assembly method, scale bar 500 nm. Reproduced with permission from [4]. Copyright American Chemical Society, 2015. (**c**) SEM micrograph of freeze-dried capsules of T4 bacteriophage/alginate water in oil emulsion in chloroform, scale bar 5 µm. (**d**) SEM and TEM micrographs (**e**) of PEO electrospun nanofiber containing T4 bacteriophage/alginate have been shown scale bars of 10 µm and 100 nm, respectively. The arrow indicates the presence of T4/alginate into the nanofiber. Reproduced with permission from [5]. Copyright John Wiley and Sons, 2013. (**f**) SEM image of the 3D printed bioceramic bone scaffold consisting of biphasic calcium phosphate with pores filled with a matrix of chitosan and RGD phage, scale bar 200 µm. Reproduced with permission from [6]. Copyright John Wiley and Sons, 2014. (**g**) SEM micrograph of porous alginate hydrogel containing TMV particles displaying interconnected channels and macropores, scale bar 100 µm. Reproduced with permission from [7]. Copyright American Chemical Society, 2012. (**h**) The TEM image of a mineralized E8-displaying phage bundle formed after 90 h incubation in the solution containing calcium and phosphate ions, scale bar 100 nm. Reproduced with permission from [8]. Copyright John Wiley and Sons, 2010. (**i**) The TEM image of the HAP-fd phage bundle with scale bar 100 nm. The circle indicates the presence of hydroxyapatite nanoparticles in the fibrous structure. Reproduced with permission from [9]. Copyright American Chemical Society, 2010.

In the human body, bone tissue regenerates to a greater extent when compared to other types of tissues. However, the regeneration process is complicated in the case of tumor resection, hip implant revision, and major fractures [10]. Pi et al. constructed a cartilage targeting gene delivery nanocomposite system by conjugating polyethylenimine (PEI) with M13 phage-displayed chondrocyte-affinity peptide (CAP), DWRVIIPPRPSA, which was isolated after two rounds of biopanning. During incubation, the phages expressing CAP showed higher affinity towards rabbit chondrocytes at 265.5-fold when compared to unmodified phages. They reported that the CAP-conjugated PEI particles had no species specificity in binding chondrocytes of rabbit and humans. Furthermore, most of the particles were found to enter chondrocytes without being trapped in ECM, which acknowledges their larger transfection efficiency [11].

T7 viral nanoparticles were explored to display two different functional peptides CARSKNKDC (CAR) and CRKDKC (CRK) to target the microvasculature of regenerating wound tissue, including skin and tendon [12]. Skin disintegration may occur in many ways, such as bruising, abrasion, hacking, burning, stabbing, and laceration. It was observed that CAR was similar to heparin-binding sites, whereas CRK was homologous to a segment of thrombospondin type I repeat. Interestingly, CAR displayed a dominant function in the early stages of skin wound healing, while CRK showed preferences in the later stages of the same process. As the terminal residues contain cysteine, the screened peptides had more feasibility to be involved in disulfide bond formation to form a molecular cycle structure. The CAR-expressing T7 phage nanoparticles had been found to appear in wound sites 100–140-fold more efficiently than the non-recombinant phage nanoparticle [13]. The biomedical application of siRNAs is minimal owing to their low absorption across the stratum corneum, a horny outer layer of skin. Hsu et al. [14] explored M13 phage (from Ph.D-C7C library) viral nanoparticle-expressing skin penetrating and cell entering (SPACE) peptide with the sequence of AC-KTGSHNQ-CG in order to reach

therapeutic macromolecules, including siRNAs, into the skin-associated cells. The in vitro physicochemical studies explored that the various macromolecules, including siRNA, penetrated across the stratum corneum into the epidermis layer of skin through the macropinocytosis pathway when the molecules were conjugated with SPACE.

A muscle binding M13 phage nanoparticle with peptide sequence ASSLNIA was identified to possess more excellent selectivity (at least five-times more) compared to the control phage nanoparticle. While investigating overall muscle selectivity on different organs, the muscle binding affinity was found to be 9–20-fold for the skeletal and 5–9-fold for cardiac muscle [15]. Sun et al. synthesized functional multivalent M13 phage (Ph.D.-7$^{TM}$ display library) nanoparticles to express RIYKGVIQA and SEEL sequences, which are found in Nogo-66, a neurite outgrowth inhibitory protein. They selectively bound negative growth regulatory protein 1 (NgR1) with electrostatic forces of repeated leucine residues, enhancing neural differentiation of pc12 cells. Hence, this specific engineered viral nanoparticle has been appreciated for its potential use in neurite tissue regeneration, including spinal cord injury, optic nerve injury, ischemic stroke, and neurodegenerative diseases [16]. Collett et al. suggested that hepatitis C virus-based nanoparticles could act as a quadrivalent vaccine to trigger humoral and cellular immune responses. They explored biophysical, biochemical, and biomechanical properties of nanoparticles using Atomic Force Microscopy and observed that glycosylation occurred on the surface of the nanoparticle with ordered packing of the core [17]. The literature reports revealed that Sendai virus vectors displaying cardiac transcription factors could efficiently reprogram both mouse and human fibroblasts into induced cardiomyocyte-like cells in vitro. In addition, they could reduce scar formation, maintaining cardiac function in myocardial infarction affected animals [18].

The phosphate tailored TMV nanoparticle was demonstrated to induce expression of osteospecific genes of rat bone marrow stem cells (BMSCs), including osteocalcin and osteopontin, when compared to unmodified TMV nanoparticles. As shown in Figure 2d–f, the enhanced cell attachment and spreading of BMSCs were observed in phosphate grafted TMV (TMV-Phos) coated Ti substrates more than TMV coated substrates after 14 days of incubation in cell culture [19].

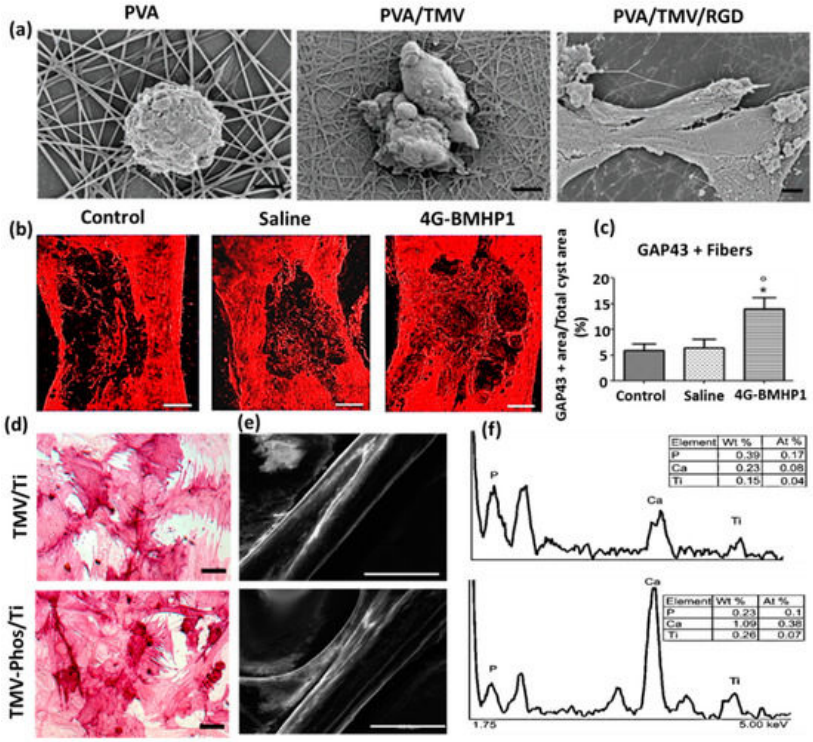


**Figure 2.** (**a**) Field emission scanning electron micrographs of Baby Hamster Kidney cells after 1 h incubation on electrospun nanofibrous substrates PVA, PVA-TMV, and PVA-TMV/RGD. Scale bar 2 µm. Reproduced with permission from [20]. Copyright John Wiley and Sons, 2014. (**b**) Immunofluorescence staining of longitudinal sections of total cyst area in spinal cord injury (SCI)-treated female Sprague-Dawley rats during the chronic phase. The synthesis of GAP-43 immunopositive fibers was significantly greater in bone marrow homing peptide-expressed phages (4G-BMHP1) treated group when compared to control groups (SCI control and saline). Scale bar 400 mm. The percentage of immunopositive fibers into the cyst area per total cyst area is represented in a bar graph (**c**) from six independent experiment results, and the values are reported with ± SEM. Significant factor * $p < 0.05$, 4G-BMHP1 vs. SCI control; 4G-BMHP1 vs. saline. Reproduced with permission from [21]. Copyright PLOS, 2011. (**d**) Bright-field optical microscope images of histochemical staining of alkaline phosphatase (ALPL) in bone marrow-derived stem cells (BMSCs) in TMV and phosphate grafted TMV (TMV-Phos)-coated Ti substrates after 14 days of culture. BMSCs have been shown to form neighboring well-spread cells

under osteogenic conditions, which are stained highly positive for ALPL. Scale bar is 100 µm. (**e**,**f**) SEM micrographs and EDX analyses of TMV and TMV-Phos coating on Ti substrates. Scale bar for SEM is 100 µm. Reproduced with permission from [19]. Copyright Elsevier, 2010.

## 2. Virus-Incorporated 2D Films and Nanofibers

A combinatorial biomaterial consisting of PVX-based cyclic RGD, containing filament (RGD-PVX) and polyethylene glycol conjugated stealth filament (PEG-PVX), was developed to analyze biodistribution in mice xenograft models. The comparative studies demonstrated that PEG-PVX was preferentially accumulated into tumor cells, while RGD-PVX was trapped into the lung site in a large quantity. It has been reported that the filamentous and elongated nanoparticles are more advantageous in drug targeting than the spherical counterparts. Non-spherical nanoparticles present more ligands on their surfaces and show significant accumulation towards the vessel wall, improving the efficiency of tumor homing. Owing to the flexible nature of viral capsid, PVX-based nanoparticles could pass through restrictions in the complex biological environments and permeate into tissue cells without difficulty [22]. Wu et al. [4] successfully synthesized TMV-based electroactive nanofibers for neural tissue regeneration from the blend of polyaniline (PANI) and sodium polystyrene sulfonate (PSS). The morphology of the TMV/PANI/PSS nanofiber has been shown through TEM micrograph in Figure 1b.

An electrospun nanofiber of blends of polyvinyl alcohol (PVA) and TMV/RGD afforded higher cell density of baby hamster kidney (BHK) cells in culture. The enhanced cell adhesion and spreading and the formation of F-actin filaments were observed more on PVA/TMV/RGD nanofiber than PVA and PVA/TMV nanofibrous substrates, which were noticed in SEM micrographs (Figure 2a). The resulting nanofiber provided electroactivity and topographical cues to the neural cells and was reported to augment the length of neurites, increase the population of cells, and lead the cellular bipolar morphology more than TMV-based non-conductive nanofibers [20]. Korehei et al. [5] produced a virus incorporated nanofiber by electrospinning the blends of polyethylene oxide (PEO) and T4 bacteriophage suspension. The SEM measurement showed that T4 bacteriophages were protected from severe electrospinning conditions, as they were concentrated within the alginate capsule, as can be seen in Figure 1c. The alginate beads containing phages were found to exhibit smooth rounded surfaces. The size of the electrospun nanofiber of PEO/alginate/T4 bacteriophages had an average diameter 500 ± 100 nm (Figure 1d). According to TEM measurement, the capsules of T4 bacteriophages were distributed without uniformity throughout the fiber matrix (Figure 1e).

The induced pluripotent stem cells (iPSCs) are a promising cell source, which can rise to different cell lineages and construct a well-developed functional bone substitute. However, there is a challenge in osteoblastic differentiation of iPSCs by a conventional biomaterial, as it may form teratoma, raising health risks. Wang et al. [23] demonstrated that a phage (M13)-based nanofiber with four different signal peptides aiming to influence stem cell fate could be potentially utilized for bone tissue regeneration. The aligned nanofibrous matrix provided biochemical and biophysical cues to the cells promoting differentiation of iPSCs into osteoblasts. Among the signal peptides investigated by them were two adhesive-directing peptides RGD and RGD/PHSRN from fibronectin, and the remaining two included ALKRQGRTLYGFGG and KIPKASSVPTELSAISTLYL sequences, which are the growth regulating peptides from osteogenic growth factor and bone morphogenetic protein 2 (BMP2), respectively. The layer-by-layer technique produced a phage-assembled nanofiber assuming nanotopography of the ridge-groove structure, wherein the phage strands were parallel to each other but separated by grooves. Due to this specialized nanotopography of material, the occurrence of controlled osteoblastic differentiation was observed, even in the absence of osteogenic supplements. The research group reported that the phages displaying growth factor signal peptides could express a higher level of alkaline phosphatase (ALP) than the phages having adhesive signal peptides on the surface. The in vivo animal studies disclosed that iPSCs alone caused teratoma after one month of cells injection into nude mice, whereas the group of iPSC-derived osteoblasts did not. Cigognini and co-workers engineered an electrospun nanofibrous scaffold dispersing phage-displayed bone marrow homing peptide (BMHP (1) with sequence PFSSTKT and investigated its potential use in a chronically damaged spinal cord, which was caused by the degeneration of the central nervous system [21]. The clinical data showed that the biomimetic material enhanced nervous tissue regeneration, owing to porosity and nanostructure at the microscopic level, and improved the locomotor recovery of experimental rats. From Figure 2b,c, the histological analyses revealed that the scaffold affected increased cellular infiltration and axonal regeneration after eight weeks of experimental investigation in rats. They found a higher synthesis of growth-associated protein 43 (GAP-43) in engineered scaffold-treated animal when compared to saline and control groups with spinal cord defects. Our research group has explored electrospun nanofibrous matrices of PLGA containing self-assembled M13 bacteriophages along with additives RGD and graphene oxide to show enhanced differentiation of fibroblasts, smooth muscle cells, and myoblasts [24][25][26][27][28].

## 3. Virus-Incorporated 3D Hydrogel Scaffolds

Cell-laden-agarose hydrogel was prepared by dispersing genetically engineered rod-shaped PVX nanoparticles, which present functional RGD peptides and mineralization inducing peptides (MIP) on its surface, into agarose polymeric components [29]. Luckanagul et al. [7] prepared freeze-dried solid foam of a porous alginate hydrogel (PAH) comprising TMV. The incorporation of TMV nanoparticles resulted in large sized and well-defined spherical pores (100–500 μm) in TMV/PAH, analyzed by Field Emission Scanning Electron Microscope image (Figure 2g).

The PVX nanoparticles adopted a nano-filamentous structural network on coated surfaces. Exploiting the synergistic effect of both peptides, the PVX nanoparticles in hydrogel expressed significant cell adhesion as well as hydroxyapatite nucleation. Confirmed by SEM and immunostaining characterizations, it was further reported that the viral nanoparticles could be preserved over 14 days in hydrogel and the whole biomaterial could act as a promising bone substitute. Maturavongsadit et al. [30] developed an injectable TMV based hydrogel under physiological conditions to imitate a cartilage microenvironment. The hydrogel was prepared by cross-linking methacrylate hyaluronic acid polymers by cysteine inserted TMV mutants involving in situ Michael addition reaction. The hydrogel was reported to influence enhancement of cartilage tissue regeneration by promoting chondrogenesis via up-regulation of BMP-2. The interaction of TMV nanoparticles with the cells assisted the high-level expression of BMP-2, an effective inducer of differentiation of mesenchymal stem cells into chondrocytes.

Luckanagul et al. [6] investigated the performance of functional TMV-RGD-blended alginate hydrogel nanocomposites to treat in vivo cranial bone defects in Sprague-Dawley rats. The TMV-functionalized sponge-like hydrogel supported cell localization without triggering any systemic toxicity in the defect area, and hence was envisaged as an active bone replacement biomimetic material in the future direction of reconstructive orthopedic surgery. Shah et al. [31] studied an integrated co-assembled hydrogel system of peptide amphiphiles, in which M13 phage coat protein was modified to express a high density of binding peptide HSNGLPL to combine with transforming growth factor β1 (TGF-β1). The research group found an enhancement in articular cartilage tissue regeneration in a rabbit model with a full-thickness chondral defect because of the slower release of growth factor from the hydrogel, with approximately 60% of cumulative drug release at 72 h, which supported the viability and chondrogenic differentiation of mesenchymal stem cells in the defective site. The in vivo evaluation of the rabbit model showed that the hydrogel treated animal group had no apparent symptoms of chronic inflammatory responses after four weeks. All of the rabbits appeared with a full range of motion in their knees at the end of the investigation. Caprini et al. [32] isolated M13 phage-displayed peptide, KLPGWSG, which could adhere on the surface of murine neural stem cells. Subsequently, the research group designed a self-assembled KLPGWSG-based biomimetic hydrogel with tunable visco-elastic properties for the regeneration of the degenerated nervous system. It was discovered that the phage-based hydrogel favored cell adherence and differentiation in the range of 100–1000 Pa, suggesting that the elastic property of the matrix is a crucial factor in tissue regeneration.

## 4. Virus-Incorporated Organic-Inorganic Hybrid Nanocomposites

The interaction of organic and inorganic biocompatible materials in scaffolds bring about significant impacts in biomedical applications. Cementum, classified as a hard mineralized tissue, surrounds tooth root and has been a part of periodontal tissue that connects the tooth to the bone. When an infectious biofilm adheres to tooth root, triggering periodontal disease, the tooth loss is more enhanced. Gungormus et al. [33] demonstrated amelogenin-derived M13 phage-displayed peptide controlled hydroxyapatite biomineralization for dental tissue regeneration. It was reported that Amelogenin directed hydroxyapatite to form a protein matrix during the formation of enamel. Hence, the research group synthesized the cementomimetic material by applying an aqueous solution of the amelogenin-displayed peptide on the human demineralized root surface to form a layer, which was subsequently immersed into the solution of calcium and phosphate ions. Ramaraju et al. [34] isolated M13 phage-displayed peptides to design a dual functional apatite-coated film for effective bone tissue regeneration. They reported that one peptide sequence of the phage, VTKHLNQISQSY, had mineral (apatite) binding affinity with 25% hydrophobicity, whereas another peptide, DPIYALSWSGMA, had cell binding affinity with 50% hydrophobicity. Also, they discovered that the dual functional apatite-based biomaterial could stimulate the adhesion strength of human bone marrow stromal cells (hMSC) and subsequently increase cell proliferation and differentiation. Due to the mineral binding affinity, the film provided a platform for the adherence of osteogenic cells with osteoconductive and osteoinductive signals. Further, the biomimetic nanocomposite showed a greater extent of proliferation of hMSCs with an elevated level of Runx2 expression when compared to biomimetic apatite without functional peptides.

Wang et al. [6] prepared a 3D-printed biomimetic nanofiber with M13 phage-displayed RGD peptides residing in the pores of the scaffold to enhance bone tissue regeneration. The nanocomposite consisted of hydroxyapatite and tri-calcium phosphate showing an ordered pattern with interconnected micro and macro scale pores, which are shown in the TEM micrograph (Figure 1f). The research group implanted a MSC-seeded biomimetic scaffold into a rat radial bone defect and discovered that the order of regeneration was found as follows: scaffold filled with modified phages > scaffolds filled with wild-type phages > pure scaffold. He et al. [8] carried out a similar kind of research work, genetically modifying M13 phage to express oligonucleotide encoding E8 and inducing self-assembly followed by oriental mineralization to synthesize nanofibrous biomimetic materials under the influence of divalent calcium ions. The resulting mineralized phage bundle has been shown in TEM micrography (Figure 1h). Wang et al. [9] used $Ca^{2+}$ ions to prompt self-assembly of fd phage-based anionic nanofibers and transform them into a bundle sheet (Figure 1i), which provided insights into biomineralization and fabrication of organic–inorganic hybrid nanocomposites. The divalent ion-triggered bundle not only acted as a biotemplate but also served as a Ca source to initiate the ordered nucleation and growth of crystalline hydroxyapatite in the biological fluid.

## References


1. Lee, K.L.; Uhde-Holzem, K.; Fischer, R.; Commandeur, U.; Steinmetz, N.F. Genetic engineering and chemical conjugation of potato virus X. Methods Mol. Biol. 2014, 1108, 3–21.
2. Li, L.; Xu, C.; Zhang, W.; Secundo, F.; Li, C.; Zhang, Z.-P.; Zhang, X.-E.; Li, F. Cargo-compatible encapsulation in virus-based nanoparticles. Nano Lett. 2019, 19, 2700–2706.
3. Sitasuwan, P.; Lee, L.A.; Li, K.; Nguyen, H.G.; Wang, Q. RGD-conjugated rod-like viral nanoparticles on 2D scaffold improve bone differentiation of mesenchymal stem cells. Front. Chem. 2014, 2, 31.
4. Wu, Y.; Feng, S.; Zan, X.; Lin, Y.; Wang, Q. Aligned electroactive TMV nanofibers as enabling scaffold for neural tissue engineering. Biomacromolecules 2015, 16, 3466–3472.
5. Korehei, R.; Kadla, J. Incorporation of T4 bacteriophage in electrospun fibres. J. Appl. Microbiol. 2013, 114, 1425–1434.
6. Wang, J.; Yang, M.; Zhu, Y.; Wang, L.; Tomsia, A.P.; Mao, C. Phage nanofibers induce vascularized osteogenesis in 3D printed bone scaffolds. Adv. Mater. 2014, 26, 4961–4966.
7. Luckanagul, J.; Lee, L.A.; Nguyen, Q.L.; Sitasuwan, P.; Yang, X.; Shazly, T.; Wang, Q. Porous alginate hydrogel functionalized with virus as three-dimensional scaffolds for bone differentiation. Biomacromolecules 2012, 13, 3949–3958.
8. He, T.; Abbineni, G.; Cao, B.; Mao, C. Nanofibrous bio-inorganic hybrid structures formed through self-assembly and oriented mineralization of genetically engineered phage nanofibers. Small 2010, 6, 2230–2235.
9. Wang, F.; Cao, B.; Mao, C. Bacteriophage bundles with prealigned Ca2+ initiate the oriented nucleation and growth of hydroxylapatite. Chem. Mater. 2010, 22, 3630–3636.
10. Luckanagul, J.A.; Metavarayuth, K.; Feng, S.; Maneesaay, P.; Clark, A.Y.; Yang, X.; García, A.J.; Wang, Q. Tobacco mosaic virus functionalized alginate hydrogel scaffolds for bone regeneration in rats with cranial defect. ACS Biomater. Sci. Eng. 2016, 2, 606–615.
11. Pi, Y.; Zhang, X.; Shi, J.; Zhu, J.; Chen, W.; Zhang, C.; Gao, W.; Zhou, C.; Ao, Y. Targeted delivery of non-viral vectors to cartilage in vivo using a chondrocyte-homing peptide identified by phage display. Biomaterials 2011, 32, 6324–6332.
12. Saidykhan, L.; Abu Bakar, M.Z.; Rukayadi, Y.; Kura, A.U.; Latifah, S.Y. Development of nanoantibiotic delivery system using cockle shell-derived aragonite nanoparticles for treatment of osteomyelitis. Int. J. Nanomed. 2016, 11, 661–673.
13. Jarvinen, T.A.; Ruoslahti, E. Molecular changes in the vasculature of injured tissues. Am. J. Pathol. 2007, 171, 702–711.
14. Hsu, T.; Mitragotri, S. Delivery of siRNA and other macromolecules into skin and cells using a peptide enhancer. Proc. Natl. Acad. Sci. USA 2011, 108, 15816–15821.
15. Samoylova, T.I.; Smith, B.F. Elucidation of muscle-binding peptides by phage display screening. Muscle Nerve 1999, 22, 460–466.
16. Sun, Z.; Dai, X.; Li, Y.; Jiang, S.; Lou, G.; Cao, Q.; Hu, R.; Huang, Y.; Su, Z.; Chen, M.; et al. A novel Nogo-66 receptor antagonist peptide promotes neurite regeneration in vitro. Mol. Cell. Neurosci. 2016, 71, 80–91.
17. Collett, S.; Torresi, J.; Earnest-Silveira, L.; Christiansen, D.; Elbourne, A.; Ramsland, P.A. Probing and pressing surfaces of hepatitis C virus-like particles. J. Colloid Interface Sci. 2019, 545, 259–268.

18. Engel, J.L.; Ardehali, R. Sendai virus based direct cardiac reprogramming: What lies ahead? Stem Cell Investig. 2018, 5, 37.
19. Kaur, G.; Wang, C.; Sun, J.; Wang, Q. The synergistic effects of multivalent ligand display and nanotopography on osteogenic differentiation of rat bone marrow stem cells. Biomaterials 2010, 31, 5813–5824.
20. Zhao, X.; Lin, Y.; Wang, Q. Virus-based scaffolds for tissue engineering applications. Wiley Interdiscip. Rev. Nanomed. Nanobiotechnol. 2015, 7, 534–547.
21. Cigognini, D.; Satta, A.; Colleoni, B.; Silva, D.; Donega, M.; Antonini, S.; Gelain, F. Evaluation of early and late effects into the acute spinal cord injury of an injectable functionalized self-assembling scaffold. PLoS ONE 2011, 6, e19782.
22. Shukla, S.; DiFranco, N.A.; Wen, A.M.; Commandeur, U.; Steinmetz, N.F. To target or not to target: Active Vs. passive tumor homing of filamentous nanoparticles based on Potato virus X. Cell. Mol. Bioeng. 2015, 8, 433–444.
23. Wang, J.; Wang, L.; Yang, M.; Zhu, Y.; Tomsia, A.; Mao, C. Untangling the effects of peptide sequences and nanotopographies in a biomimetic niche for directed differentiation of iPSCs by assemblies of genetically engineered viral nanofibers. Nano Lett. 2014, 14, 6850–6856.
24. Han, J.; Devaraj, V.; Kim, C.; Kim, W.G.; Han, D.W.; Hong, S.W.; Kang, Y.C.; Oh, J.W. Fabrication of self-assembled nanoporous structures from a self-templating M13 bacteriophage. ACS Appl. Nano Mater. 2018, 1, 2851–2857.
25. Shin, Y.C.; Lee, J.H.; Jin, L.; Kim, M.J.; Oh, J.W.; Kim, T.W.; Han, D.W. Cell-adhesive RGD peptide-displaying M13 bacteriophage/PLGA nanofiber matrices for growth of fibroblasts. Biomater. Res. 2014, 18, 14.
26. Shin, Y.C.; Lee, J.H.; Jin, O.S.; Lee, E.J.; Jin, L.H.; Kim, C.S.; Hong, S.W.; Han, D.W.; Kim, C.; Oh, J.-W. RGD peptide-displaying M13 bacteriophage/PLGA nanofibers as cell-adhesive matrices for smooth muscle cells. J. Korean Phys. Soc. 2015, 66, 12–16.
27. Shin, Y.C.; Lee, J.H.; Jin, L.; Kim, M.J.; Kim, C.; Hong, S.W.; Oh, J.W.; Han, D.W. Cell-adhesive matrices composed of RGD peptide-displaying M13 bacteriophage/poly(lactic-co-glycolic acid) nanofibers beneficial to myoblast differentiation. J. Nanosci. Nanotechnol. 2015, 15, 7907–7912.
28. Shin, Y.C.; Kim, C.; Song, S.J.; Jun, S.; Kim, C.S.; Hong, S.W.; Hyon, S.H.; Han, D.W.; Oh, J.W. Ternary aligned nanofibers of RGD peptide-displaying M13 bacteriophage/PLGA/graphene oxide for facilitated myogenesis. Nanotheranostics 2018, 2, 144–156.
29. Lauria, I.; Dickmeis, C.; Roder, J.; Beckers, M.; Rutten, S.; Lin, Y.Y.; Commandeur, U.; Fischer, H. Engineered Potato virus X nanoparticles support hydroxyapatite nucleation for improved bone tissue replacement. Acta Biomater. 2017, 62, 317–327.
30. Maturavongsadit, P.; Luckanagul, J.A.; Metavarayuth, K.; Zhao, X.; Chen, L.; Lin, Y.; Wang, Q. Promotion of in vitro chondrogenesis of mesenchymal stem cells using in situ hyaluronic hydrogel functionalized with rod-like viral nanoparticles. Biomacromolecules 2016, 17, 1930–1938.
31. Shah, R.N.; Shah, N.A.; Del Rosario Lim, M.M.; Hsieh, C.; Nuber, G.; Stupp, S.I. Supramolecular design of self-assembling nanofibers for cartilage regeneration. Proc. Natl. Acad. Sci. USA 2010, 107, 3293–3298.
32. Caprini, A.; Silva, D.; Zanoni, I.; Cunha, C.; Volonte, C.; Vescovi, A.; Gelain, F. A novel bioactive peptide: Assessing its activity over murine neural stem cells and its potential for neural tissue engineering. New Biotechnol. 2013, 30, 552–562.
33. Gungormus, M.; Oren, E.E.; Horst, J.A.; Fong, H.; Hnilova, M.; Somerman, M.J.; Snead, M.L.; Samudrala, R.; Tamerler, C.; Sarikaya, M. Cementomimetics-constructing a cementum-like biomineralized microlayer via amelogenin-derived peptides. Int. J. Oral Sci. 2012, 4, 69–77.
34. Ramaraju, H.; Miller, S.J.; Kohn, D.H. Dual-functioning peptides discovered by phage display increase the magnitude and specificity of BMSC attachment to mineralized biomaterials. Biomaterials 2017, 134, 1–12.